International Geology Review
Publication details, including instructions for authors and subscription information:
http://www.tandfonline.com/loi/tigr20

New geological and geochronological data of the Placer de Guadalupe uplift, Mexico: a new piece of the Late Triassic-Jurassic Nazas Arc?

Janet Villarreal-Fuentes[a], Gilles Levresse[a], Angel F. Nieto-Samaniego[a] & Rodolfo Corona-Esquivel[b]

[a] Centro de Geociencias, Universidad Nacional Autónoma de México, Querétaro, México
[b] Instituto de Geología, Universidad Nacional Autónoma de México, México City, México

Published online: 11 Dec 2014.

International Geology Review, 2014
Vol. 56, No. 16, 2000–2014, http://dx.doi.org/10.1080/00206814.2014.984353

New geological and geochronological data of the Placer de Guadalupe uplift, Mexico: a new piece of the Late Triassic–Jurassic Nazas Arc?

Janet Villarreal-Fuentes[a], Gilles Levresse[a]*, Angel F. Nieto-Samaniego[a] and Rodolfo Corona-Esquivel[b]

[a]*Centro de Geociencias, Universidad Nacional Autónoma de México, Querétaro, México;* [b]*Instituto de Geología, Universidad Nacional Autónoma de México, México City, México*

(*Received 11 August 2014; accepted 27 October 2014*)

Basement exposed in the Placer de Guadalupe–Plomosas uplift in northern Mexico provides important clues for the geologic evolution of the region. The stratigraphic units form stacked thrust sheets of psammitic and calcareous formations, interlayered with magmatic rock. The eastern calcareous and quartzite formations exhibit structures associated with ductile deformation, whereas the upper stratigraphic units only contain structures formed via younger brittle deformation. Porphyry interlayered in the upper Plomosas Formation has a U-Pb zircon age of 171 ± 1 Ma. This age is consistent with its stratigraphic position, interbedded quartzarenites with a maximum depositional age of ~168 Ma. Granite flakes within the Horquilla Formation are dated at 209 ± 3 Ma, and the La Viñata quartzite exhibits a maximum age of ~193 Ma. The Upper Plomosas Formation correlates well with the arc-related Middle Jurassic Nazas Formation of northeastern Mexico, constituting the first report of a Jurassic continental margin arc outcrop in the 'Central Mexican Gap zone'. We document Late Norian to Bajocian ages for the stratigraphic units cropping out in the Placer de Guadalupe area. The Jurassic age cluster indicates that the Nazas Arc magmatism in the region occurred during the Late Triassic and ended in the Middle Jurassic times. Permian ages previously assigned to these rocks and the occurrence of a Permo–Triassic deformation event have to be dismissed.

Keywords: Placer de Guadalupe–Plomosas uplift; Mexico; U-Pb dating; Nazas Arc; Jurassic

Introduction

The geologic evolution of northern Mexico involves the superposition of various orogenic events (Figure 1), resulting in a range of Late Palaeozoic to Neogene geological features. The thrust-belt of the Marathon–Ouachita orogen and the Triassic to Jurassic Nazas magmatic arc are key elements in the region (Poole *et al.* 2005; Stern and Dickinson 2010; Barboza-Gudiño *et al.* 2013; among others). Younger features, such as the Late Cretaceous–Palaeogene Laramide orogen and the Oligocene Sierra Madre Occidental (SMO) volcanic province, obscure the link between the eastern and western segments of the Nazas Arc, resulting in the Central Mexican Gap (Figure 1; Ferrari *et al.* 2005). Detailed field work and precise geochronology are needed to decipher the complex geologic history of this region.

The Placer de Guadalupe–Plomosas uplift in the state of Chihuahua hosts the first uranium mine in North America in 1868 (Gonzales Reyna 1946), yet the geologic evolution of the Plomosas uplift remains poorly resolved (Bridges 1962; Boucot and Johnson 1968; Hennings 1994; Haenggi 2001; Goodell and Feinstein 2008; Barboza-Gudiño *et al.* 2013; among others). Despite the scientific and economic importance of the Guadalupe–Plomosas uplift, studies of this geological feature of Chihuahua are scarce, and detailed information is limited to the mining district (Krieger 1932; Gonzales Reyna 1946; Bridges 1962, 1964; Boucot and Johnson 1968; Goodell and Feinstein 2008). Geochemical studies are absent, and geochronological data are scarce, unreliable, and usually refer to specific sites, with the results extrapolated over the entire range (Wells 1930; Ramírez and Acevedo 1957; De Cserna *et al.* 1968; Montgomery 1997b). Consequently, the genesis and evolution of the Guadalupe–Plomosas uplift remains unclear. For example, there is no agreement on the time and geological context of the formations in the uplift or their geological significance. Most of the formations are composed of conglomerate, sandstone and shale, which do not favour reliable geochronological determinations (Bridges 1962).

We present new U-Pb geochronologic data for granite and subaerial acid volcanics (porphyry), and detrital zircons in sandstone and quartzite from the Guadalupe–Plomosas uplift in Chihuahua. Our results indicate the existence of a Jurassic arc instead of Permian foreland sedimentary formations. The Permo–Triassic deformation event has to be dismissed in favour of a more traditional pre-Laramide North American Cordilleran orogenic evolution.

*Corresponding author. Email: glevresse@gmail.com

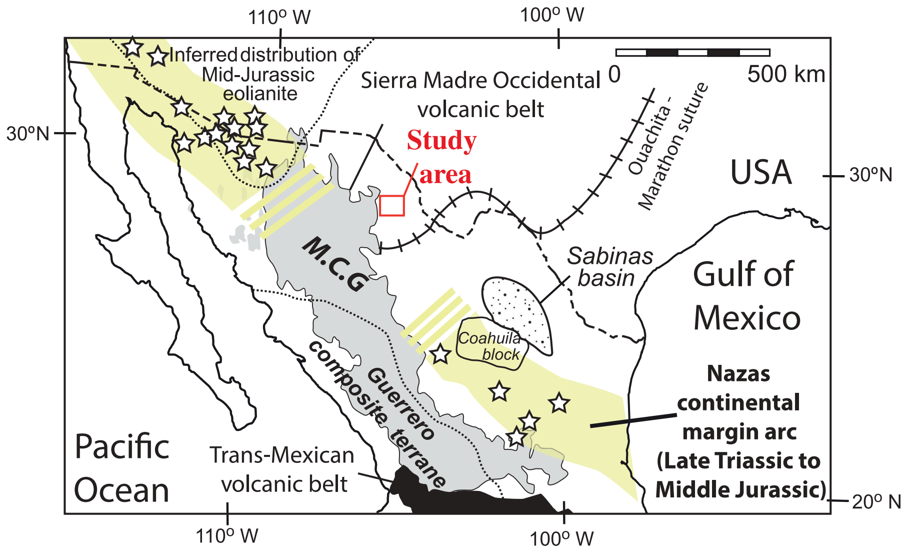

Figure 1. Location map illustrating the trend of the Jurassic continental margin arc through Mexico and the study area location (modified from Lawton and Molina 2014). Open stars on the map refer to Jurassic U-Pb age localities and 'M.C.G' M.C.G is defined as the Mexico Central gap (see Lawton and Molina 2014). Sierra Madre Oriental and Trans-Mexican belt shape a are taken from Ferrari *et al.* (2005). The Ouachita Marathon orogenic belt is taking from Poole *et al.* (2005).

Geological setting

The Plomosas–Placer de Guadalupe uplift is located in the central part of the Chihuahua Fold Belt and represents the eastern margin of the Chihuahua basin. The region is characterized by a succession of endorheic basins and ranges. The ranges are formed by Late Jurassic to Late Cretaceous sedimentary rocks folded during the Laramide orogeny and are covered by undeformed Paleogene volcanic sequences (Figures 1 and 2). The basins were filled by Paleogene volcanic flows and Paleogene to Recent detrital sediment. Paleogene volcanic rocks in the area are dated from ca. 46 Ma to ca. 27.5 Ma (Cameron *et al.* 1989 and references therein; McDowell and Mauger 1994) and are considered part of the SMO volcanic province (Megaw 1990; McDowell *et al.* 1997; Paz Moreno *et al.* 2003; Ferrari *et al.* 2005 and references therein; Oviedo-Patron *et al.* 2010). The first Eocene volcanic flows rest uncomformably on Mesozoic rocks at a low dip angle (King and Adkins 1946; Ferrari *et al.* 2005 and references therein; Oviedo-Patron *et al.* 2010). Their emplacement is attributed to the succession of extensional events during Eocene–Oligocene time (McDowell and Mauger 1994; Ferrari *et al.* 2005 and references therein).

In this regional geologic context, the Plomosas–Placer de Guadalupe area includes distinctive geological characteristics, such as Proterozoic to Palaeozoic strata (De Cserna *et al.* 1968; Torres *et al.* 1999), a diverse rock record that includes Neoproterozoic metamorphic rocks (954.7 ± 4 Ma, Ar-Ar in hornblende, Iriondo *et al.* 2004; Mauger *et al.* 1983), and Palaeozoic calcareous and siliciclastic sedimentary formations. The uplift is also characterized by westward-vergent thrust faults which verge in the opposite direction of the typical Laramide deformation structures (Bridges 1962; Hennings 1994; Goodell and Feinstein 2008). Campa-Uranga and Coney (1983) and Barboza-Gudiño *et al.* (2013) proposed that the Palaeozoic sedimentary formations are related to the Laurentian passive margin development. The Palaeozoic series forms a succession of calcareous and sandstones formations known as the El Paso, Cable Canyon, Montoya, Percha, Escabrosa Paradise, and Horquilla formations. All of these formations contain mid-Ordovician to Pennsylvanian fauna. In particular, the Horquilla Formation is characterized by abundant crinoid stems and fusulinids (*fusulina* aff., *Fusulinella* sp., *Wedekindllina*, Pennsylvanian in age, Bridges 1964). The stratigraphically overlying Lower Plomosas Formation includes limestone with bryozoan fragments to marl (Ramírez and Acevedo 1957). The Lower Plomosas Formation Carboniferous age is determined by crinoids (Ramírez and Acevedo 1957; Montgomery 1997a) and cross-cutting dioritic dikes (317 ± 16 Ma; K-Ar in hornblende, Montgomery 1997b). The Upper Plomosas Formation includes siliciclastic to conglomerate rock with interstratified volcanic flows dated 270 Ma (Plomo Alfa; De Cserna *et al.* 1968) and is overlain by shale and sandstone of the Green Formation. Finally, the La Casita Formation is Kimmeridgian in age, is overlain upon the Green Formation (King and Adkins 1946), and is composed of intercalations of sandstone in lutites. Intrusive bodies mapped in the area were not described and are assumed to be Paleogene in age (see Figure 2, Mauger *et al.* 1981; Gonzalez Ramirez 2005). From NW to SE, the main ranges in which these strata crop out are the Placer de Guadalupe, the Monillas, the Plomosas, the Sofia, and the Carrizalillo ranges (Figure 2).

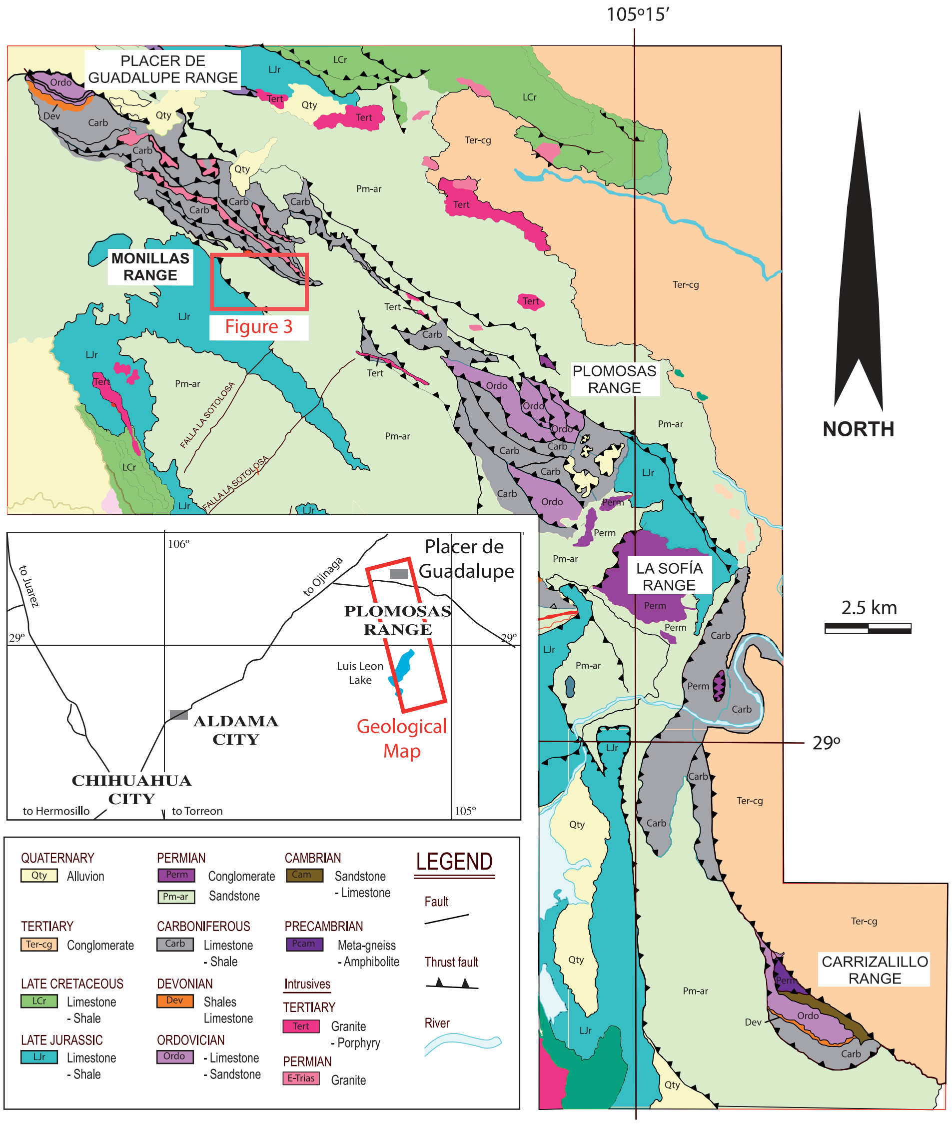

Figure 2. Detailed geological map of the eastern Sierra de los Cuarzos area, (modified from the Placer de Guadalupe and Plomosa cartography; Consejo de Recursos Minerales (CRM) 1976).

All of these formed from NW–SE-striking thrusts with a southwestward transport direction (Hennings 1994; Haenggi 2001).

Different models have been proposed for formation of the Plomosas-Placer de Guadalupe area. Bridges (1962) and Barboza-Gudiño *et al.* (2013) proposed Permo–Triassic compression, generating thrusts and recumbent folds with tectonic transport to the west. Goodell and Feinstein (2008) suggest a model of ‘kink band’ structure that involves a series of tear faults with two stages of deformation: the first occurred during the Permian–Triassic period (Late Ouachita orogen), and the second occurred during the Late Cretaceous and early Palaeocene related to the Laramide orogeny. Hennings (1994) and Haenggi (2001) preferred a model of propagation containing an anticline with reverse fault tectonic transport in a single deformation stage during the Laramide orogeny.

Analytical techniques

Petrography

Magmatic and sedimentary mineralogy was documented through field observations and petrographic and scanning electron microscopy (SEM) analyses. Mineral phases were identified with a SEM-EDX at the Laboratorio de Geofluidos in the Centro de Geociencias, Universidad Nacional Autónoma de México, Querétaro, México (CGEO).

Zircon separation

Rock samples from the granitic flakes, porphyry, and sedimentary formations were collected from five locations

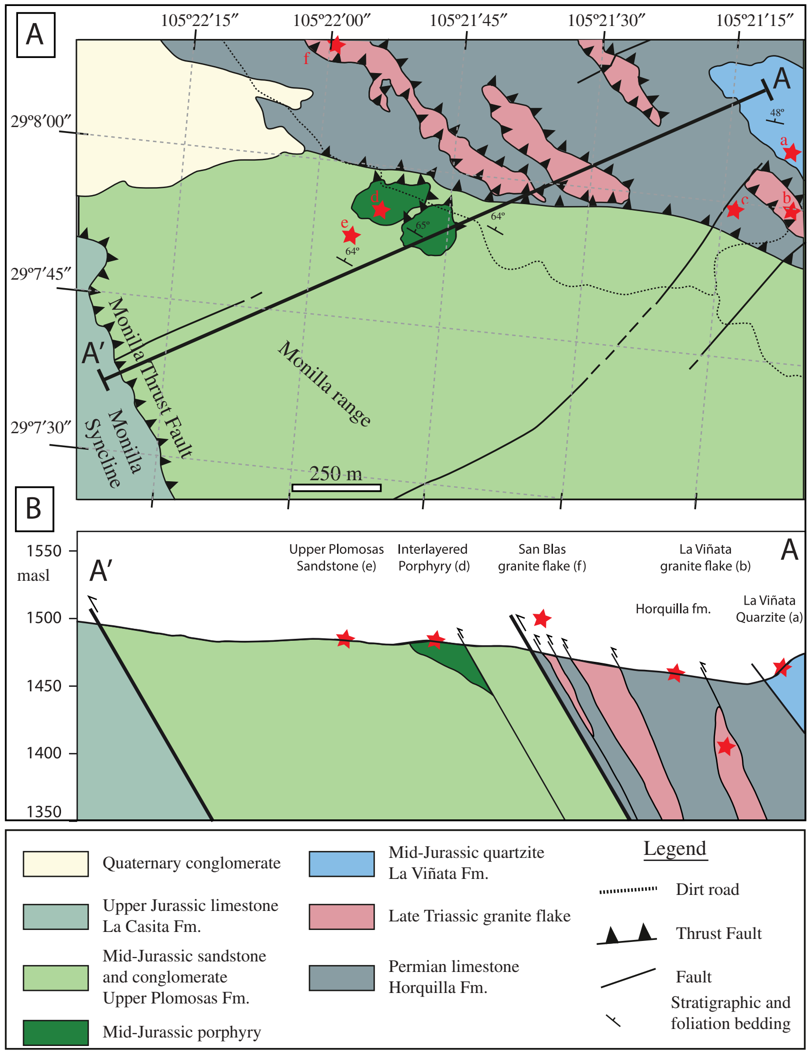

Figure 3. Geologic map of the study area. Sample locations are indicated by red stars. See Figure 1 for map location. (a) La Viñata quartzite; (b) La Viñata granite flake; (c) Horquilla limestone formation; (d) Interlayered porphyry; (e) Upper Plomosa sandstone; (f) San Blas granite flake.

shown in Figure 3 (red stars). The samples were crushed, powdered and sieved (200 to 50 mesh). Heavy mineral fractions were obtained by density preconcentration in methylene iodide. The non-magnetic fraction was separated with a Franz isodynamic magnet. Final zircon separates were randomly hand-picked under a binocular microscope, mounted in epoxy resin together with a standard (National Institute of Standards and Technology (NIST)), and subsequently polished. Laser ablation target points were selected on cathodoluminescence images in order to identify zircon cores and overgrowth zones.

U-Pb age dating

The zircon samples were analysed at the laser ablation facility at Laboratorio de Estudios Isotópicos (LEI), Centro de Geociencias, UNAM. The instrument consists of a Resonetics excimer laser ablation workstation (Solari *et al.* 2010), coupled with a Thermo XII Series quadrupole ICPMS. The laser ablation workstation operates a Coherent LPX 200, 193 nm excimer laser and an optical system equipped with a long-working-distance lens with 50–200 μm focus depth. The ablation cell is pressurized with He and is capable of fast signal uptake and washout. The ablation pit was 34 μm diameter, and the pit depth during the analysis is about 20–25 μm, for a total mass ablated during each analysis of ~70–80 ng. Seventeen isotopes are scanned during each analysis, allowing a quantitative measurement of those isotopes necessary for U-Pb dating (lead, uranium, and thorium), as well as detailed monitoring of major and trace elements such as Si, P, Ti, Zr and rare earth elements (REEs), which can yield important information on the presence of microscopic inclusions in the zircons (e.g. monazite, apatite, or titanite) that produce erroneous age results. For each analysis, 25 s of signal background are monitored, followed by 30 s of signal with laser firing with a frequency of 5 Hz and an energy density of ~8 J/cm^2 on target. The remaining 25 s is for washout and stage repositioning. We analysed natural zircon standards for mass bias correction and for calculation of down-hole and drift fractionation, as well as NIST standard glass to recalculate U and Th concentrations in zircon.

Geological and petrological description

The study area forms an E–W transect that is 2.5 km long by 1 km wide, located 4 km south of the town of Placer de Guadalupe (Figure 3). To the northeast, the study area includes the upper contact between the Horquilla Formation with the La Viñata quartzite and ends to the southwest at the Monillas thrust fault, which juxtaposed the upper Plomosas Formation above the Jurassic calcareous formation. Rocks in the study area include a succession of siliciclastic to carbonate sedimentary formations with different degrees of metamorphism and volcanic and plutonic intrusions (Figure 4). All of the contacts observed between the different formations are marked by ~N30ºW thrust faults (see Figures 2 and 3). In the following, we present a macroscopic and petrographic description of each formation encountered along the E–W transect (see Figures 3 and 5).

In the east, the La Viñata quartzite is a tectonic flake of 150 m thickness within the calcareous Permian Horquilla Formation. Individual quartzite beds are 10–30 cm thick, with a grainy texture showing a reddish-brown weathering surface and a white fresh fracture surface. It is a recrystallized quartz arenite with >70% quartz crystals that are rounded to sub-rounded, and scarce oxidized lithic clasts. The interstitial matrix exhibits a high degree of oxidation (see Figure 5A, A′ and A″). The lower contact is tectonic and sub-parallel to the La Viñata quartzite bedding planes (N66°W/48°NE).

The contact between the La Viñata quartzite sliver and the calcareous Horquilla Formation (also known as the Pastor Formation) is covered by young sediments and could not be directly observed. The Horquilla Formation is grey metamorphosed and recrystallized limestone that is strongly ductilely deformed. Deformation is manifested by sigma structures and microfolds and an intense penetrative foliation. Crinoid stems occur in a sparry matrix and shear zones are visible in thin section (see Figure 5B, B′ and B″). The crinoids suggest a Pennsylvanian to Wolfcampanian age (Bridges 1964; Montgomery 1997b, 2004).

Several other tectonic flakes, granitic in composition, appear into the Horquilla Formation (notably the San Blas and La Viñata flakes among others, see Figure 3). These were suggested to be mid-Triassic in age based on field relationships (Hernàndez-Noriega and García-Peralta 2005). A few metres west of the La Vinata quartzite is a 100 m-thick granitic flake that forms part of a major intrusion (more than 2 km long and ~150 m thick). Both upper and lower contacts with the Horquilla Formation are t-ectonic. The granite exhibits a pink–white weathering colour and grey-coloured fresh fracture surfaces. The macroscopic texture is porphyritic with phenocrysts of

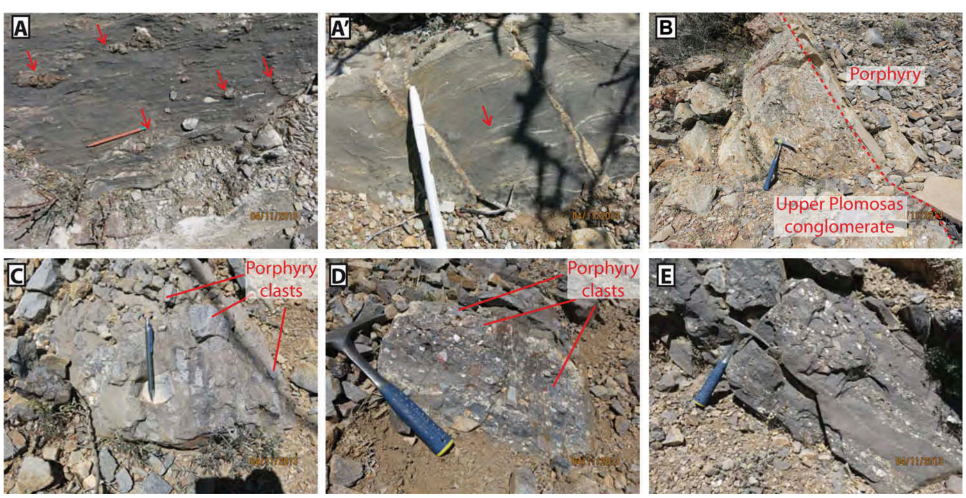

Figure 4. (A and A′): Photographs of ductile deformation in the Horquilla Formation (A, rolling structures; A′, recumbent isoclinal folds). (B) Field photography of the erosional contact between the interlayered prophyry (~171 Ma) and the Upper Plomosa sandstone (~168 Ma). (C, D and E) Evolution of the conglomerate composition from the porphyry contact (B) to the Upper Plomosa sandstone (E). The conglomerate evolution is from a very coarse non-transported conglomerate composed of 100% angular porphyry clasts of pluri-centimetre size (C) to a coarse transitional conglomerate with 20% angular porphyry clasts *versus* 80% rounded quartz, limestone and rock fragments of centimetre size (D) finally to the classical Upper Plomosa medium conglomerate without a trace of any porphyry clasts (E).

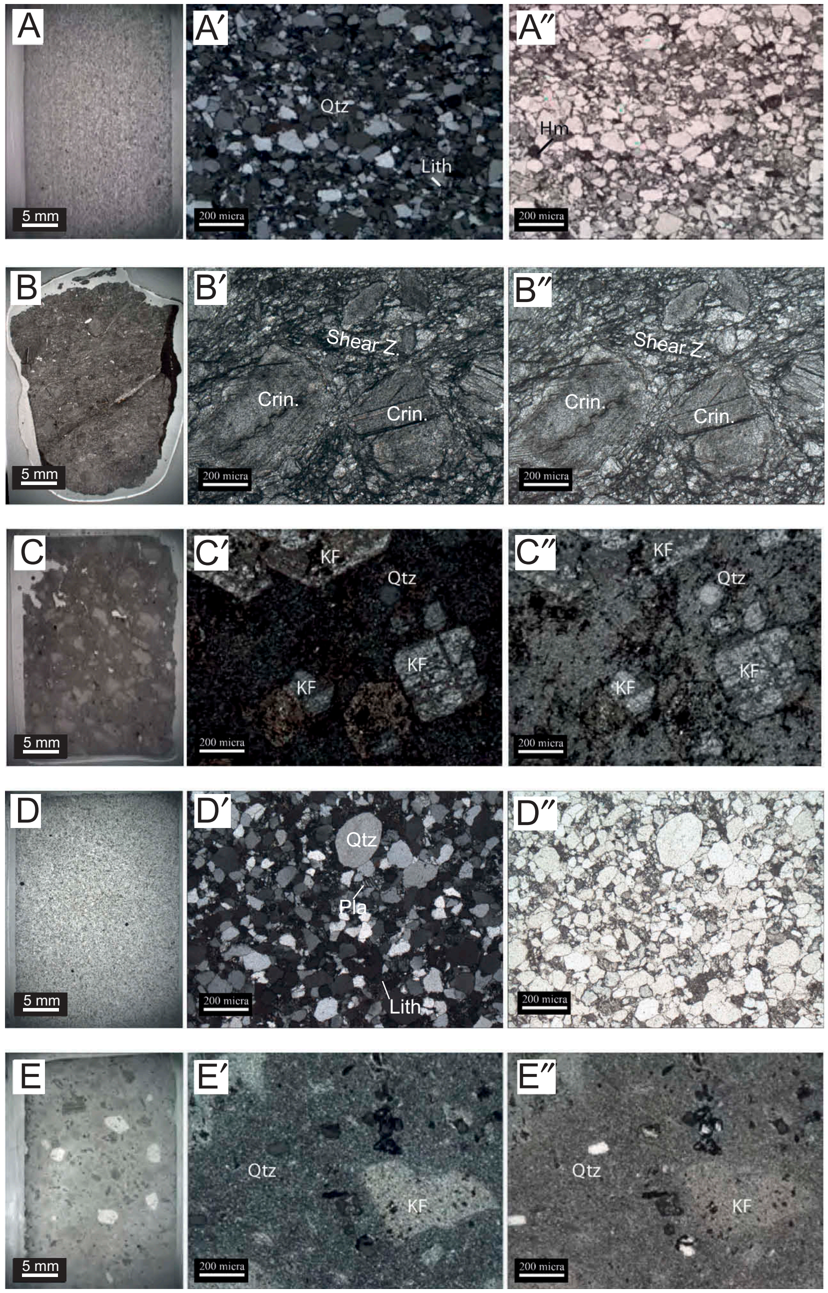

Figure 5. (A, A′, and A″) La Viñata quartzite: (A) photomicrograph with plane polarized light of thin section, (A′) photomicrograph with plane polarized light, and (A″) same as A′ with crossed nicols. (B, B′, and B″) Horquilla Formation: (B) photomicrograph with plane polarized light of thin section, (B′) photomicrograph with plane polarized light, and (B″) same as B′ with crossed nicols. (C, C′, and C″) La Viñata granite flake: (C) photomicrograph with plane polarized light of thin section, (C′) photomicrograph with plane polarized light, and (C″) same as C′ with crossed nicols. (D, D′, and D″) Upper Plomosa sandstone: (D) photomicrograph with plane polarized light of thin section, (D′) photomicrograph with plane polarized light, and (D″) same as D′ with crossed nicols. (E, E′, and E″) Interlayered prophyry: (E) photomicrograph with plane polarized light of thin section, (E′) photomicrograph with plane polarized light, and (E″) same as E′ with crossed nicols. Definitions are: Qtz, quartz; Lith, lithic fragment; Hm, haematite; KF, potassic feldspar; Crin, crinoid stem; Shear Z, shear zone; Pla, plagioclase.

quartz and plagioclase. The phenocrysts are dominated by K-feldspar (30–45%) and resorbed quartz (rounded edges and some crystals show reaction aureole with the matrix, see Figure 5C, C′ and C″). These have varying sizes ranging from millimetres to centimetres (for the single crystals and aggregates, respectively). The matrix and plagioclase phenocrysts exhibit slight alteration (sericitization and oxidation).

The footwall of the Horquilla Formation thrust is dominated by sandstone and conglomerate in upward-coarsening intervals within the upper Plomosas Formation. It is characterized by a grey to reddish weathering surface and a dark grey fresh fracture surface with beds of variable thicknesses ranging from 5 to 60 cm. This same formation is observed until the Monillas thrust fault (the main thrust fault) over the Monilla Jurassic anticline. The formation ranges from ~400- to 500 m thick over the study area. Although not directly dated, regional correlation and the stratigraphic position of the Upper Plomosas Formation suggest a late Permian age (de Cserna *et al.* 1968). Strata trend N60°W/64°NE, with fracturing parallel to the bedding and joints in the direction N26°E/vertical and N80°W/62°SW.

The sandstone is quartzarenite, with 85% quartz, 10% lithic, and less than 5% plagioclase with a texture that is equigranular with angular to sub-rounded grains. Additionally, the grains appear to be supported grain to grain (Figure 5D, D′ and D″). In the Dickinson (1985) provenance diagram, the Upper Plomosa Formation plots in the recycled orogenic field.

A volcanic rhyolitic flow is interlayered in the Upper Plomosas sandstone series. The upper contact is tectonic and sub-parallel to the Upper Plomosas bedding planes (N60°W/64°NE). This contact is highlighted by magnetite and quartz cement along the stratigraphic plane. The lower contact is an erosional contact with the stratigraphic sequence inverted. The rhyolitic/sedimentary transition initiates with monogenic and angular rhyolitic clast conglomerate, and breccia that changes to thin alternating sandstone and fine conglomerate (Figure 4). At the microscopic scale, the lava flow exhibits a porphyritic texture, with phenocrysts of quartz, potassium feldspar (orthoclase) and rare plagioclase (Figure 5 E, E′ and E″). The edges of the quartz exhibit corrosion. The feldspar and plagioclase phenocrysts show seritization. Some of the quartz and feldspar crystals are fractured (see Figure 5 E, E′ and E″). The microcrystalline matrix is formed by silica, and a flow texture around some phenocrysts is observed.

Magmatic geochemistry

In order to define the rock types and their geodynamical context, we analysed major and trace elements in the dated granite flakes, as well as the interlayered-porphyry samples. The results are presented in Appendix 1 (see online supplemental material at http://dx.doi.org/10.1080/00206814.2014.984353).

In the total alkalies–silica (TAS) diagram, the La Viñata and San Blas granite flake plot in the quartz-monzonite field (with a SiO_2 content of ~65% and ~2.3% K_2O) and the K_2O/Na_2O ratio (~0.4) is typical of the medium K calc-alkaline series. Geotectonically, the samples are classified as volcanic arc granites (Pearce *et al.* 1984). Relatively low Rb/Zr ratios (~0.7) and Nb concentrations (~20 ppm) further indicate a normal calc-alkaline continental arc (Brown 1994). Chondrite-normalized (Sun and McDonough 1989) REE patterns illustrate that granite flakes display a fractionation from light REE (LREE) to middle REE (MREE) ($8.9 < (La/Yb)_N < 10.8$), a general absence of any Eu anomalies and a slight fractionation from MREE to heavy REE (HREE) ($1.5 < (Gd/Yb)_N < 1.7$) with a concave-upward shape.

The interlayered porphyry, within the Upper Plomosas Formation, is classified as rhyolite and belongs to the high-K calc-alkaline series ($K_2O > 7\%$) as defined by Peccerillo and Taylor (1976). The porphyry has high silica content of ~75 wt. % (normalized to 100% volatile-free) and is peraluminous (A/CKN: 1.02). The REE patterns display a slight fractionation from LREE to HREE $(La/Yb)_N = 10.1$, strong Eu anomalies (Eu/Eu* = 37) and a flat pattern from MREE to HREE $(Gd/Yb)_N = 1.3$. Such characteristics are typical for other high-silica rhyolites (Mahood and Halliday 1988; Orozco-Esquivel *et al.* 2002; Murray 2013).

Geochronology

When possible, geochronological studies were carried out to locate different formations in a coherent stratigraphic column. Additionally, in order to correlate the sandstone formations, grain populations were evaluated, and all grain analyses were combined into composite probability distributions (Dickinson and Gehrels 1995). The results are presented in Figures 5 and 6 and Appendix 2 (see online supplemental material at http://dx.doi.org/10.1080/00206814.2014.984353).

Detrital Zircon Ages

For the La Viñata quartzite, 116 analyses provide a dispersion of $^{206}Pb/^{238}U$ ages from 2290 ± 27 Ma to 193 ± 3 Ma. Five analyses were removed as a result of high discordance (defined as >20% discordant and identified in blue in Figures 6) between the $^{206}Pb/^{238}U$ and $^{207}Pb/^{235}U$ ages. The remaining 111 results are divided into six main grain-age populations (see Figures 6 and 7) that are separated by age gaps exceeding the 1σ error of the individual grains in the adjacent populations. The recognized grain-age populations are distributed from 1400 to 1450 Ma (seven zircons), 1150 to 1250 Ma (15 zircons), 1000 to 1100 Ma (20 zircons), 600 to 700 Ma (seven zircons), 350 to 500 Ma (17 zircons) and 250 to 300 Ma (seven zircons). The maximum depositional age of the La Viñata quartzite is 193 ± 3 Ma, based on the youngest single zircon age, although a more conservative estimate is ~245 Ma (Early Triassic), which was encountered in seven zircons grains.

Ninety-nine analyses were performed on the Upper Plomosas sandstone zircon grains, all within accordance limit (minimum 80%). The ages obtained show wide

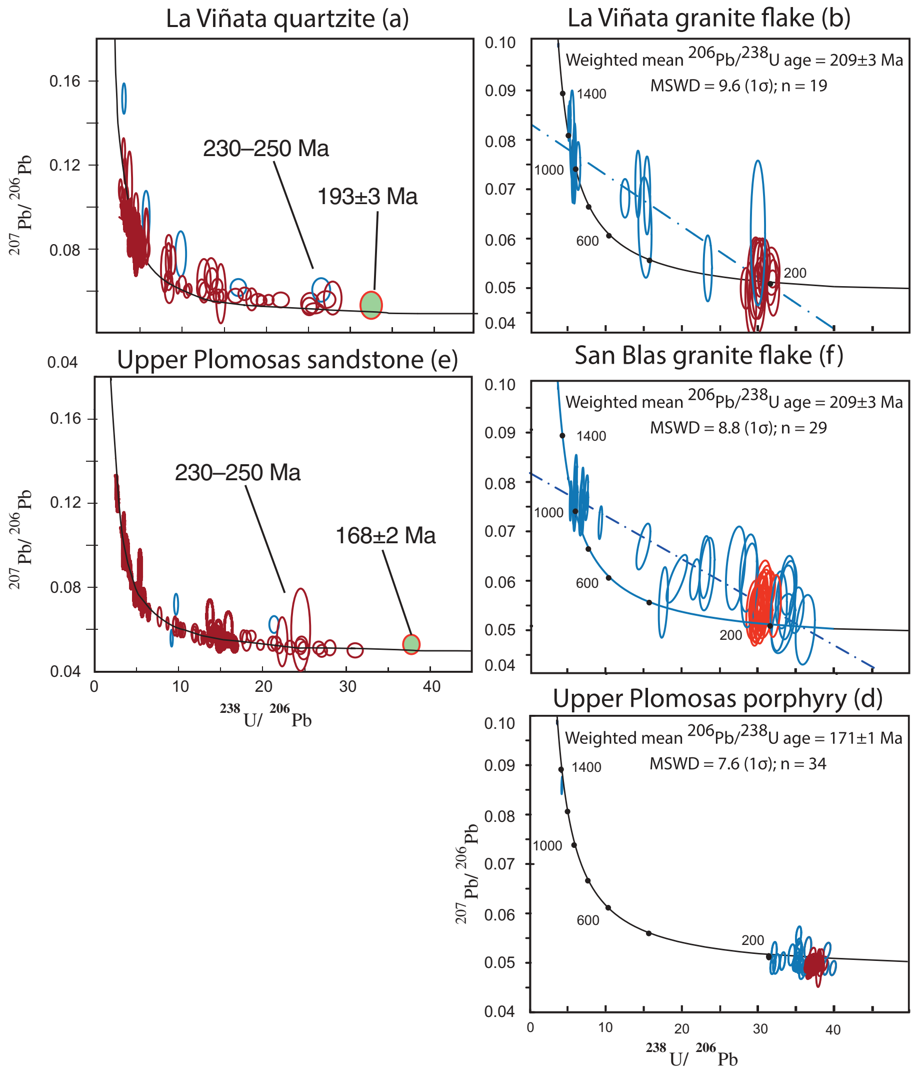

Figure 6. Tera–Wasserburg diagrams for the U-Pb isotope of zircons from the La Viñata quartzite, the La Viñata and San Blas granite flakes, the Upper Plomosa sandstone, and the interlayered porphyry within the Upper Plomosa sandstone. Diagrams, ages and errors (1s) were generated using the Isoplot 3.71 program (Ludwig 2008). The green ellipses correspond to the youngest single zircon ages. The red ellipses represent the analysis used for the determination of the crystallization ages (right column) and age populations (left column).

dispersion from 2747 ± 25 Ma to 168 ± 2 Ma (see Figures 6 and 7). The statistical distribution of different grain-age populations allows the determination of four clusters of ages ranging from 1000 to 1100 Ma (20 zircons), 600 to 700 Ma (eight zircons), 350 to 500 Ma (23 zircons) and 250 to 300 Ma (14 zircons). The youngest zircon, representative of the maximum deposition age, has a reported age of 168 ± 2 Ma. Until ~256 Ma, no well-defined peak is close (see Figures 6 and 7).

Igneous Rock U-Pb Ages

The dated magmatic formations are from the Upper Plomoza Formation and La Viñata–San Blas granites as thrusted ‘flake’ within the Carboniferous Horquilla Formation (see Figures 3 and 5). The magmatic ages are presented in a Tera–Wasserburg plot, and the weighted mean ages were calculated from grain-age groups with a 2σ error, such that the mean square weighted deviation (MSWD) is as close to unity as possible. Both magmatic events incorporated older grains at some point in their history, as indicated by the presence of older grains in each sample. In the Upper Plomosas porphyry, the older zircon grains are characterized by a rounded shape.

The 54 analyses carried out on zircon grains from the Upper Plomosas porphyry yield $^{206}Pb/^{238}U$ ages ranging from 1354 ± 9 Ma to 160 ± 1 Ma. Three analyses were discarded due to their high discordance (>20%), or because of their $^{206}Pb/^{238}U$ and $^{206}Pb/^{238}U$ discordant ages. Thirty-

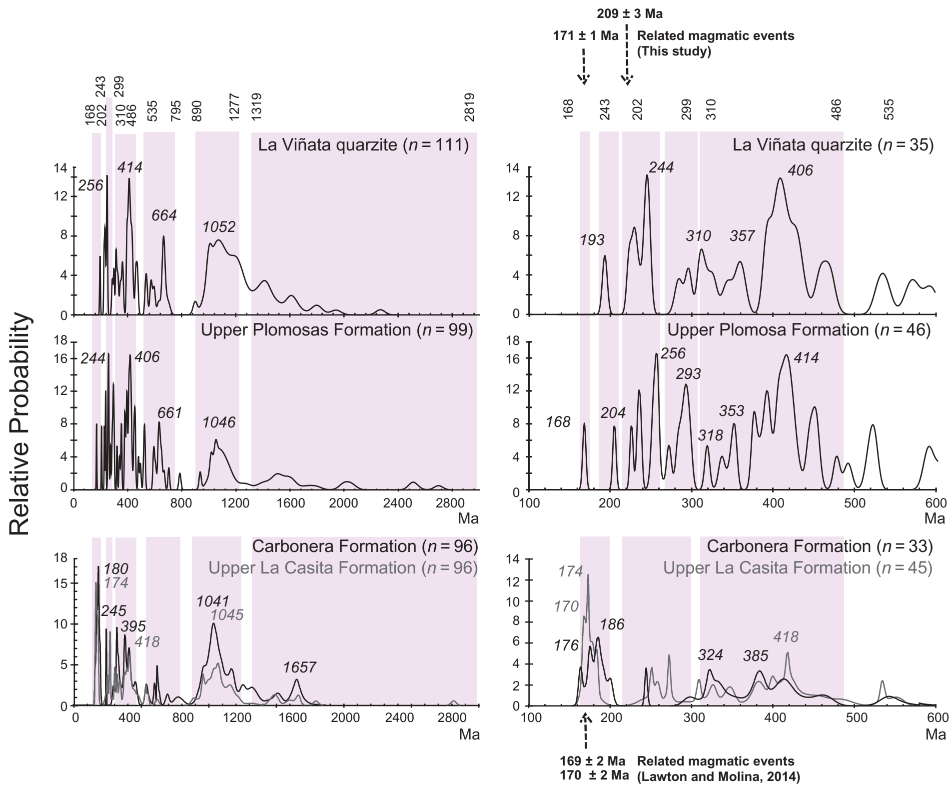

Figure 7. Age-probability spectra for the individual detrital-zircon samples. Left column: all grains. Right column: grains younger than 600 Ma. The above curves indicate age peaks in Ma. Arrows and ages marked in bold denote the interlayered volcanism events in Ma. For comparison, we present the age-probability spectra of the Carbonara and Upper Casita Formations, modified from Lawton and Molina (2014).

four of the remaining 51 analyses form the youngest tight cluster (shown in red within Figure 6). These data yielded a weighted mean $^{206}Pb/^{238}U$ crystallization age of 171 ± 1 Ma (*n* = 34, MSWD of 7.6, Ludwig 2008). Twenty older zircon grains yielded concordant ages scattered between 1354 ± 9 Ma and 180 ± 1 Ma. These older grains could be explained by various scenarios: (1) as xenocrysts acquired by the assimilation of older crust material, (2) as antecrysts remobilized from only slightly older Jurassic magma chamber material, or (3) as detrital grains entrained during surface volcanic rock emplacement.

For La Viñata–San Blas Granites flake, 37 analyses carried out from both samples provide $^{206}Pb/^{238}U$ ages ranging from 2103 ± 64 Ma to 199 ± 2 Ma and 1111 ± 10 Ma to 183 ± 2 Ma, respectively. Only one analysis in the San Blas sample and three in the La Viñata sample were discarded due to high discordance (>20%). In the San Blas granite, 29 analyses were conducted to determine the remaining 36 concordant $^{206}Pb/^{238}U$ ages, which formed a tight cluster at the lower age. The weighted mean crystallization age (Ludwig 2008) is 209 ± 3 Ma (*n* = 29, MSWD of 8.8, see Figure 6). In the La Viñata granite, 19 analyses conducted for the remaining 34 concordant $^{206}Pb/^{238}U$ ages form a tight cluster at the lower age. The weighted mean crystallization age (Ludwig 2008) is 209 ± 3 Ma (*n* = 19, MSWD of 9.6, see Figure 6).

In the Tera–Wasserburg plot (see Figure 6) both of the granite samples show an older cluster formed by concordant ages between 965 ± 18 Ma and 1190 ± 51 Ma. These older grains could be explained using various scenarios, as previously mentioned in the porphyry section. Between ~230 Ma and ~900 Ma in both samples, very few analyses (with higher discordance, but still lower than 20%) are distributed along a discordia line connecting the younger (~230 Ma) and the older (~1000 Ma) clusters. The lower clusters intersect an age of 205 ± 13 Ma, which is in agreement with the weighted mean crystallization age. These ages are performed in zircon grains showing a perfect external shape but an inner inherited core and are interpreted as a mixing of the ages of the inherited core and late magmatic rims.

Discussion

Local stratigraphy revision

The contacts between each formation are mainly thrust faults. The studied column is composed of a tectonic flake stack without any geochronological continuum, which does not permit a description of a coherent stratigraphic column. However, some relevant geochronological and field information were obtained.

- The assignment of a Pennsylvanian age to the Horquilla Formation is based on evidence from the crinoid fragments. The crinoids, shape alteration by high intensity deformation combined with absence of other fossils do not allow a confident stratigraphic age assignment. Crinoids have been described in Mexico from the Permian to Late Jurassic (Peck 1948; Simms 1986; Esquivel-Macías *et al.* 2005). In the study area, the Horquilla Formation is part of a tectonic stack without defined stratigraphic relationship, so it could also be Permian to Jurassic in age.
- The different granite flakes within the Horquilla Formation exhibit comparable chemical compositions and the same crystallization age. These flakes clearly represent the same rocks, and no rocks of such age are known in the region.
- The interlayered porphyry crystallization age is calculated at 171 ± 1 Ma. This age places an upper limit on the age of the Upper Plomosa Formation in the studied stratigraphic column. At the regional scale, the interlayered porphyry crystallization age overlaps within the age error of the ignimbrite flows interlayered within the Nazas sedimentary formation (170 ± 2 Ma and 170 ± 2 Ma, single zircon crystal, Stern and Dickinson 2010; Lawton and Molina 2014, see Figure 7). This material also shares the same whole rock chemistry characteristics (high siliceous and K calc alkaline series with a high Eu anomaly, Bartolini *et al.* 2003).
- The Upper Plomosas Formation was sampled over a few metres stratigraphically above the contact with the interlayered porphyry and ideally to the inverted stratigraphic sequence so that the samples have ages younger than 171 ± 1 Ma. For the Upper Plomosas Formation, the youngest zircon, representative of the maximum age of deposition, has a reported age of 168 ± 2 Ma, and there is no defined peak until ~256 Ma. Only the youngest zircon age (168 ± 2 Ma) is coherent with the sample stratigraphic position and is interpreted by the authors as the Upper Plomosas Formation maximum age of deposition. The first defined peak suggests the outcropping of Permian plutonic rocks already recognized in the close area (Carrizalillo: 267 ± 21 Ma, K-Ar microcline, Aldama: 250 ± 20 Ma, K-Ar microcline, Torres *et al.* 1999) and more generally in northern Mexico (Lawton and Molina 2014; Ocampo-Díaz *et al.* 2014). The Nazas magmatic system, including the La Viñata and San Blas granitic flakes, seem not to have experienced erosion during the Upper Plomosas Formation deposition. Compared to the sedimentary formations hosting the Carbonera Middle Jurassic ignimbrite flow, the Upper La Casita, the Nazas (Lawton and Molina 2014) and the Upper Plomosas Formations exhibit a comparable maximum age of deposition (~170–176 Ma).
- The maximum depositional age for the La Viñata quartzite is 193 ± 3 Ma, based on the youngest single zircon age. A more conservative estimation could be represented by an ~245 Ma peak (Early Triassic). No geological field evidence permits the determination of the most realistic age. Compared with the Upper Plomosas and the Carbonera Formations, the Upper La Casita and the Nazas Formations (Lawton and Molina 2014, Figure 7), all of the sedimentary formations exhibit comparable grain-age population distributions from the Mesoproterozoic (1100–1000 Ma) to Lower-Mid Jurassic (168–193 Ma) periods. The authors interpret this common evolution from the Mesoproterozoic to Lower-Mid Jurassic in a local way as the youngest single zircon age (193 ± 3 Ma) should be a more representative age for the La Viñata quartzite. Additionally, in a regional way all of the formations exhibit the same geochronological evolution in a similar geodynamic context over a comparable period of time.

The crystallization ages of the granite flake (209 ± 3 Ma) and interlayered porphyry (171 ± 1 Ma), as well as the detrital zircon ages of the La Viñata quartzite (193 ± 3 Ma), the Upper Plomosa sandstone (168 ± 2 Ma) and the Horquilla Formation are Late Triassic to Middle Jurassic in age (Figure 8). Therefore, we can definitively discard the previous Permian age interpretation suggested for these formations (De Cserna *et al.* 1968). The position of these formations and their relationship in the regional stratigraphic column should be modified, in particular the relation between the Upper Plomosas and La Casita Formations (Figure 8).

The Upper Plomosas Formation and its interlayered porphyry exhibit a comparable maximum depositional/crystallization age and grain-age population distribution to the Nazas arc volcano sedimentary formations, including the La Casita Formation (Lawton and Molina 2014, see Figure 7). The whole rock chemistry of the Late Triassic granite flake and the Middle Jurassic porphyry are characteristic of calc-alkaline continental arc and confirm an established magmatic arc from at least ~210 to ~170 Ma, which is termed the Nazas Arc in north-central Mexico (Figure 8). The Upper Plomosas Formation represents the first documented outcrops of the Nazas Arc in the Main Central Gap (MCG) (Figure 1). The upper Plomosas and La Casita geochronological equivalence strongly suggest than the Upper Plomosas Formation represent the basal continental member of the La Casita Formation (Figure 8).

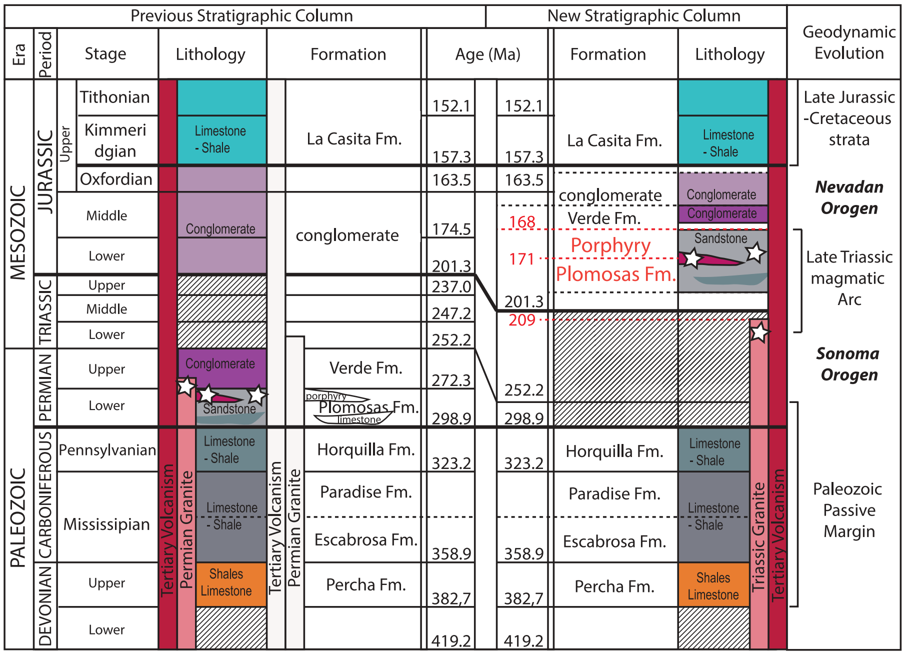

Figure 8. Statigraphic column of the Plomosas–Placer de Guadalupe uplift area. The left column is modified from the Consejo de Recursos Minerales cartography, and the right column is proposed according to the new isotopic ages. The boundaries of geochronologic units are those proposed in the International Chronostratigraphic Chart (Cohen *et al.* 2013). Open stars indicate sample locations. Colour and lithology are the same as in Figure 2.

The deformation (foliation and schistosity) in all of the formations is controlled by the Monilla main thrust (~N30ºW). Additionally, the deformation intensity is not homogenous along the studied column. The Upper Plomosas Formation exhibits pervasive schistosity, whereas the Horquilla Formation and the La Viñata quartzite show high grades of metamorphism, including recrystallization and ductile domain deformation. This deformation dichotomy suggests that the different formations followed different pathways during their tectonic emplacement. The Horquilla Formation and La Viñata quartzite have the deepest pathway and probably reach a depth of 15 km (Rutter 1974, 1995).

The deformation in the Upper Plomosas Formation is subtler and the bedding, schistosity and tectonic contacts are sub-parallel to the Monilla thrust fault (~N30ºW). The relationship between the Upper Plomosas Formation and the interlayered porphyry suggests an inverted stratigraphic sequence. The porphyry footwall is characterized by a sedimentary contact and on the top by a tectonic contact (see Figure 2, thrust, ~N60ºW). The Upper Plomosa Formation represents the lower flank of the recumbent isoclinal thrust fold spilled to the west and eroded.

Regional geodynamical implication

The new geochronological data obtained in this work has important implications for our understanding of northern Mexico geological evolution (Figures 1 and 8). Previously, the volcanic and sedimentary formations that form the Plomosas–Placer de Guadalupe range were interpreted as a Marathon orogen foreland basin. Our new data indicate that formations of Permian age do not crop out in the study area. The outcropping units are related to Late Triassic to Jurassic magmatic arc development (Figure 8). Most formation models proposed for the Plomosas–Placer de Guadalupe area involve a Permian–Triassic deformation event (Bridges 1962; Goodell and Feinstein 2008; Barboza-Gudiño *et al.* 2013), which is contradicted by our new geochronological data (Figure 8). These two-event models should not be discarded, but rather should be re-evaluated to include younger orogenic events.

In Figures 8 and 9, we propose a new geodynamic evolution sequence from the Palaeozoic to Late Jurassic based on our observations. During the Palaeozoic, the study area was part of the southern Pangea passive margin (Sanchez-Zavala *et al.* 1999; Keppie *et al.* 2004). Palaeozoic and Permian sedimentary formations were deposited on the continental platform from subtidal to deep ocean conditions (Centeno-García 2005). The gap in the sedimentary record from the Pennsylvanian to Upper Triassic corresponds in age with the Sonoma orogen described in western Pangea (270–240 Ma; Drewes 1981; Domeier and Torsvik 2014). The Sonoma orogeny occurrence is in agreement not only with the sediment deposition gap and the Permian formation erosion but also with the occurrence of reverse faults with opposite vergence, which we interpret as formed during tectonic

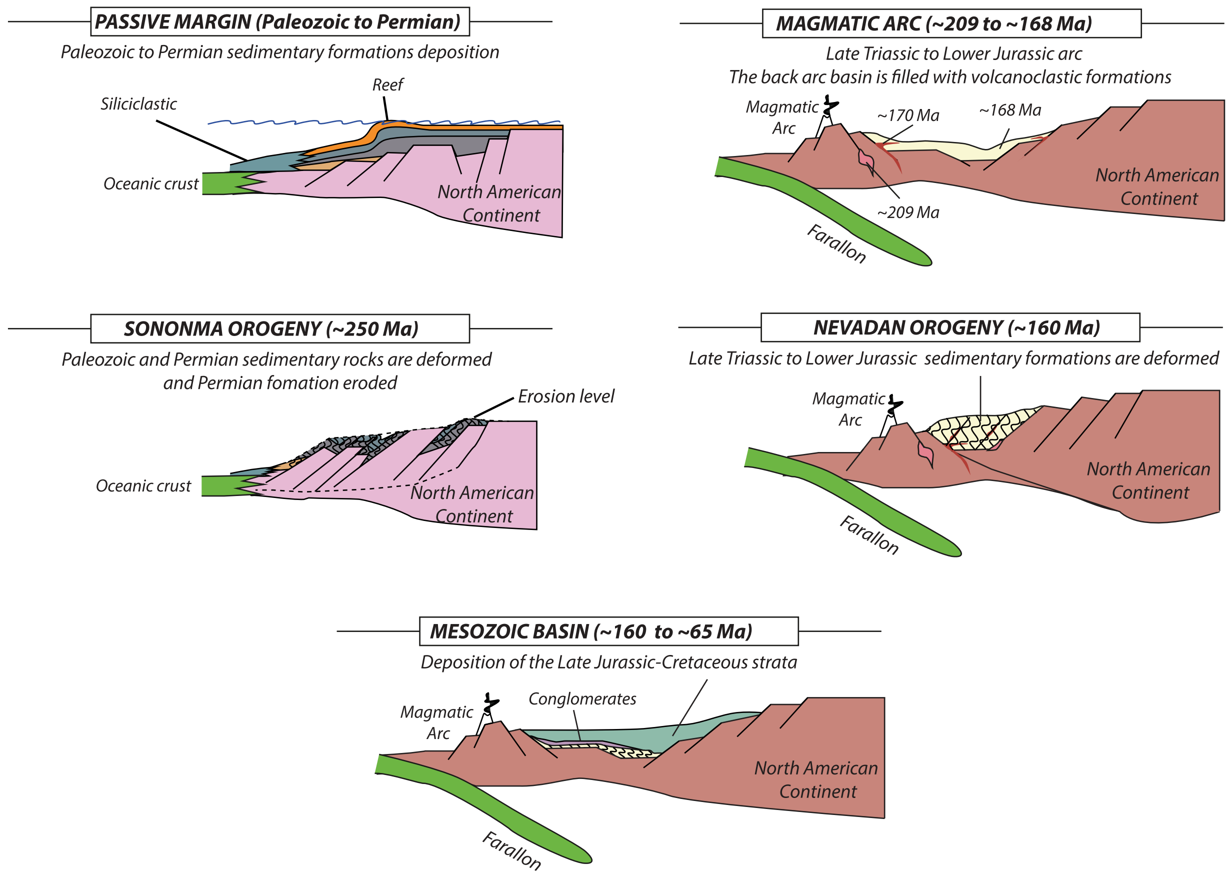

Figure 9. Tecono-stratigraphic evolution of the Placer de Guadalupe uplift from the Palaeozoic to the Late Jurassic. During the Palaeozoic, the study area forms the southern continental platform of Pangea. Sedimentary formations are deposited from subtidal to deep ocean conditions. The gap in the sedimentary record from the Permian to Upper Triassic illustrates the occurrence of the Sonoma orogen (~250 Ma). Triassic granites are the first evidence of the Late Triassic to Middle Jurassic magmatic arc building. The magmatic arc presence is confirmed by the siliciclastic Upper Plomosas Formation deposition (~168 Ma) and its interbedded volcanism (~170 Ma). The conglomerate sequences laying locally between the Upper Plomosas and the La Casita Formations, and the two deformations in the Upper Plomosas Formation support the evidence of the Nevadan orogen occurrence. The Late Jurassic La Casita Formation initiates the deposition of the uninterrupted sedimentary Mesozoic column that was later deformed during the Laramide orogen.

lateral expulsion in an orogenic border system (e.g. Agard *et al.* 2010; Domeier and Torsvik 2014). The Upper Triassic granites at ~210 Ma are the first evidence of the beginning of a subduction system and the formation of a Late Triassic to Middle Jurassic magmatic arc (this study). This magmatic arc was sustained at least until Middle Jurassic time (~170 Ma). The volcano-siliciclastic upper Plomosas formation filled a juvenile back arc basin with material mainly coming from the mainland, containing Lower Jurassic, Upper Triassic, Permian, Devonian to Upper Ordovician, Upper Neoproterozoic, Upper Mesoproterozoic, and Neoarchean detrital zircons. The magmatic arc sedimentary formations recorded two deformations of types ductile (crystal-plastic) and brittle. A second partial sedimentary gap is recorded in the sedimentary column, from Middle Jurassic (~170 Ma) to Kimmeridgian time. This gap corresponds in age to the Nevadan orogeny within the North American cordilleran history (Ingersoll and Schweicker 1986). During this period local continental conglomerates, of small lateral dimensions and unknown ages, overlay unconformably the Upper Plomosas Formation (Gonzalez Ramirez 2005). These conglomerates are clearly unconformable on the Upper Plomosas Formation and do not reflect ductile deformation, suggesting a post-Nevadan orogenic origin. Unconformably overlaying these conglomerates and locally directly on the Upper Plomosas Formation was deposited the Upper Jurassic La Casita Formation. This sedimentary formation initiates a continuous cycle of calcareous deposition during all of the remainder of Mesozoic time. This long extension period ending with the Laramide orogeny (Late Cretaceous), which was characterized by a thin skin tectonic style and the reactivation of Sonoma and Nevadan faults.

Conclusions

New U-Pb ages from porphyry interlayered in the Upper Plomosas Formation, granite flake and detrita zircons from Jurassic sedimentary formations exposed in the Placer de Guadalupe area, Chihuahua, Mexico, improve our understanding of the Sierra Plomosas stratigraphy and formation. Furthermore, these new results highlight the Late Triassic–Jurassic continental margin arc outcrops in the MCG for the first time. Key insights into the new geochronology of the Placer de Guadalupe are as follows.

- The porphyry interlayered in the Upper Plomosas sandstone is dated at 171 ± 1 Ma.
- The granite flake within the Horquilla Formation is dated at 209 ± 3 Ma.
- Based on the single zircon age, the maximum deposition ages for the Upper Plomosas Formation and the La Viñata quartzite are 168 ± 2 Ma and 193 ± 3 Ma, respectively.
- Sedimentary and volcanic events, age, and petrography are comparable to the Carbonera and La Casita sedimentary formations and their related volcanic events, including the two closer outcrops of the Nazas Arc magmatism in Central Mexico.
- The occurrence of a Permo–Triassic deformation event in the Placer de Guadalupe area must be dismissed and the role of Sonoma and Nevadan orogenic events in the region should be reconsidered.

Acknowledgements

Special thanks to Carlos Ortega Obregón, Marina Vega and Teresa Soledad medina Malagon for their assistance at the CGEO laboratory. Reviews by Robert J. Stern, Claudio Bartolini, and Kathy Surpless greatly improved our presentation.

Funding

This study was financed by the UNAM-PAPIIT project [IN110912] and CONACyT projects [81584 and 80142].

Supplemental data

Supplemental data for this article can be accessed at http://dx.doi.org/10.1080/00206814.2014.984353.

References

Agard, P., Searle, M.P., Alsop, G.I., and Dubacq, B., 2010, Crustal stacking and expulsion tectonics during continental subduction: P-T deformation constraints from Oman: Tectonics, v. 29, p. 1–19. doi:10.1029/2010TC002669.

Barboza-Gudiño, J.R., Torres-Hernández, J.R., and Villasuso-Martínez, R., 2013, Estratigrafía y evolución tecónica de la Sierra Plomosas, Chihuahua, *in* Delgado, L., and Perez, L., eds., GEOS: Mexico DF, Unión Geofísica Mexicana, GET-5.

Bartolini, C., Lang, H., and Spell, T., 2003, Geochronology, geochemistry, and tectonic setting of the Mesozoic Nazas arc in north-central Mexico, and its continuation to north South America, *in* Bartolini, C., Buffler, R.T., and Blickwede, J.F., eds., The Circum Golf of Mexico and the Caribbean: Hydrocarbon Habitats, Basin Formation and Plate Tectonics: American Association of Petroleum Geologists Memoir, v. 79, p. 427–461.

Boucot, A.J., and Johnson, J.G., 1968, Devonian brachiopods from the Mina Plomosas-Placer de Guadalupe area, Chihuahua, Mexico, and their paleogeographic significance, West Texas Geological Society, Field Trip Guidebook.

Bridges, L.W., 1962, Geology of Mina Plomosa area, Chihuahua, Mexico [Ph.D. thesis]: Austin, University of Texas at Austin.

Bridges, L.W., 1964, Stratigraphy of Mine-Plomosas-Placer de Guadalupe area, *in* Geology of Mina Plomosas-Placer de Guadalupe area, Field Trip Guideb: Chihuahua, West Texas Geological Society, v. 64–50, p. 50–59.

Brown, M., 1994, The generation, segregation, ascent and emplacement of granite magma: The migmatite to crustally derived granite connection in thickened orogens: Earth-Science Reviews, v. 36, p. 83–130. doi:10.1016/0012-8252(94)90009-4.

Cameron, K.L., Nimz, G.J., Kuentz, D., Niemeyer, S., and Gunn, S., 1989, Southern Cordilleran basaltic andesite suite, southern Chihuahua, Mexico: A link between Tertiary continental arc and flood basalt magmatism in NorthAmerica: Journal of Geophysical Research, v. 94, p. 7817–7840, doi:10.1029/JB094iB06p07817.

Campa-Uranga, M.F., and Coney, P.J., 1983, Tectono-stratigraphic terranes and mineral resource distributions in Mexico: Canadian Journal of Earth Sciences, v. 20, p. 1040–1051. doi:10.1139/e83-094.

Centeno-García, E., 2005, Review of Upper Paleozoic and Lower Mesozoic stratigraphy and depositional environments of central and west Mexico: Constraints on terrane analysis and paleogeography, *in* Anderson, T.H., *et al.*, eds., The Mojave-Sonora megashear hypothesis: Development, assessment, and alternatives: Geological Society of America Special Paper, v. 393, p. 233–258.

Cohen, K.M., Finney, S.C., Gibbard, P.L., and Fan, J.X., 2013, The International Chronostratigraphic Chart: Episodes, v. 36, p. 199–204.

Consejo de Recursos Minerales (CRM), 1976, Carta geológico-minera Placer de Guadalupe H13-C48 Chihuahua, *in* Secretaria de Comercio y Fomento Industrial. 1 hoja: Pachuca, Servicio Geologico Mexicano.

De Cserna, Z., Rincón-Ortega, C., Solorio, M.J., and Schmitter, V.E., 1968, Una edad Pérmica Temprana de la región de Placer de Guadalupe, Noroeste de Chihuahua: Boletín de la Sociedad Geológica Mexicana, v. 31, no. 1, p. 65–73.

Dickinson, W.R., 1985, Interpreting provenance relation from detrital modes of sandstones, *in* Zuffa, G.G., ed., Provenance of Arenites: NATO ASI Series: Dordrecht, Reidel Publishing Company, p. 333–363, vols C 148, D.

Dickinson, W.R., and Gehrels, G.E., 1995, Detrital zircon provenance of Cambrian to Triassic miogeoclinal and eugeoclinal strata in Nevada: American Journal of Science, v. 295, p. 18–48, doi:10.2475/ajs.295.1.18.

Domeier, M., and Torsvik, T.H., 2014, Plate tectonics in the late Paleozoic: Geoscience Frontiers, v. 5, p. 303–350, doi:10.1016/j.gsf.2014.01.002.

Drewes, H.D., 1981. Tectonics of southeastern Arizona: USGS Professional Paper 1144.

Esquivel-Macías, C., León–Olvera, R.G., and Flores–Castro, K., 2005, Caracterización de una nueva localidad fosilífera del Jurásico Inferior con crinoides y amonites en el centro oriente de México. (Temapá–Hidalgo): Revista Mexicana de Ciencias Geológicas, v. 22, no. 1, p. 97–114.

Ferrari, L., Valencia-Moreno, M., and Bryan, S., 2005, Magmatismo y tectónica en la Sierra Madre Occidental y su relación con la evolución de la margen occidental de Norteamérica: Boletin de la Sociedad Geológica Mexicana, v. LVII, p. 3.

Gonzales Reyna, J., 1946, Los criaderos de uranio y oro en Placer de Guadalupe y Puerto del Aire, estado de Chihuahua: Boletin Del Consejo De Recursos Naturales No Renovables, Mexico, v. 5, p. 235.

Gonzalez Ramirez, H.F., 2005, Geologia y tectonica de Placer de Guadalupe, Chihuahua y su relación con la evolucion geodinamica de Norteamerica [Engeneering thesis]: Chihuahua, Universida Autonoma de Chihuahua.

Goodell, P.C., and Feinstein, N.M., 2008, A simulated 43-101 document of the Plomosa Property: Chihuahua, Reporte para Compañia Retec Guaru, S.A. de C.V., p. 36.

Haenggi, W.T., 2001, Tectonic history of the Chihuahua trough, Mexico and adjacent USA, Part I: The pre-Mesozoic setting: Boletín de la Sociedad Geológica Mexicana, v. LIV, p. 28–66.

Hennings, P.H., 1994, Structural transect of the southern Chihuahua fold belt Between Ojinaga and Aldama, Chihuahua, Mexico: Tectonics, v. 13, p. 1445–1460. doi:10.1029/94TC00800.

Hernández-Noriega, L., and García-Peralta, A.A., 2005, Carta geológico-minera Placer de Guadalupe H13-C48: Chihuahua: Pachuca, Hgo., Servicio Geológico Mexicano, escala 1:50,000.

Ingersoll, R.V., and Schweicker, R.A., 1986, A plate-tectonic model for Late Jurassic Ophiolite Genesis, Nevadan orogeny and forearc initiation, northern California: Tectonics, v. 5, p. 901–912. doi:10.1029/TC005i006p00901.

Iriondo, A., Kunt, M., and Winick, J.A., y CRM, 2004, $^{40}Ar/^{39}Ar$ Dating Studies of Minerals and Rocks in various areas in Mexico: USGS/CRM Scientific Collaboration (Part II). Technical report, USGS, open file report.

Keppie, J.D., Sandberg, C.A., Miller, B.V., Sánchez-Zavala, J.L., Nance, R.D., and Poole, F.G., 2004, Implications of Latest Pennsylvanian to Middle Permian Paleontological and U-Pb SHRIMP Data from the Tecomate Formation to Re-dating Tectonothermal Events in the Acatlán Complex, Southern Mexico: International Geology Review, v. 46, 8, p. 745–753. doi:10.2747/0020-6814.46.8.745.

King, R.E., and Adkins, W.S., 1946, Geology of a part of the lower Conchos Valley, Chihuahua, Mexico: Geological Society of America Bulletin, v. 57, p. 275–294, doi:10.1130/0016-7606(1946)57[275:GOAPOT]2.0.CO;2.

Krieger, P., 1932, An association of gold and Uraninite from Chihuahua, Mexico: Economic Geology, v. 27, p. 651–660. doi:10.2113/gsecongeo.27.7.651.

Lawton, F., and Molina, R.S., 2014, U-Pb geochronology of the type Nazas Formation and superjacent strata, northeastern Durango, Mexico: Implications of a Jurassic age for continental-arc magmatism in north-central Mexico: Geological Society of America Bulletin. doi:10.1130/B30827.1.

Ludwig, 2008, Isoplot/EX version 3.0, A geochronological toolkit for Microsoft Excel: Berkeley, CA, Berkeley Geochronology Center Special Publication.

Mahood, G.A., and Halliday, A.N., 1988, Generation of high-silica rhyolite: A Nd, Sr, and O isotopic study of Sierra La Primavera, Mexican Neovolcanic Belt: Contributions to Mineralogy and Petrology, v. 100, 2, p. 183–191, doi:10.1007/BF00373584.

Mauger, R., 1981, Geology of the middle part of the Calera del Nido Block, Chihuahua, Mexico, *in* Goodell, P.C., ed., Studies in Geology: Houston, TX, AAPG, v. 13.

Mauger, R.L., McDowell, F.W., and Blount, J.G., 1983, Grenville-age Precambrian rocks of the Los Filtros area near Aldama, Chihuahua, Mexico, *in* Clark, K.F., and Goodell, P.C., eds., Geology and mineral resources of north-central Mexico: El Paso Geological Society, Field Conference Guidebook, p. 165–168.

McDowell, F.W., and Mauger, R.L., 1994, K-Ar and U-Pb zircon chronology of late Cretaceous and Tertiary magmatism in central Chihuahua State, Mexico: Geological Society of America Bulletin, v. 106, p. 118–132. doi:10.1130/0016-7606(1994)106<0118:KAAUPZ>2.3.CO;2.

McDowell, F.W., Roldán-Quintana, J., and Amaya-Martínez, R., Amaya-Martínez, 1997, Interrelationship of sedimentary and volcanic deposits associated with Tertiary extension in Sonora, Mexico: Geological Society of America Bulletin, v. 109, p. 1349–1360. doi:10.1130/0016-7606(1997)109<1349:IOSAVD>2.3.CO;2.

Megaw, P.K.M., 1990. Geology and geochemistry of the Santa Eulalia mining district, Chihuahua, Mexico [Ph.D. thesis]: Tucson, University of Arizona, 463 p.

Montgomery, S.L., 1997a, Permian Bone Spring formation: Sandstone play in the Delaware Basin, part I - slope: American Association of Petroleum Geologists Bulletin, v. 81, no. 8, p. 1239–1258.

Montgomery, S.L., 1997b, Permian Bone Spring formation: Sandstone play in the Delaware Basin, part II - basin: American Association of Petroleum Geologists Bulletin, v. 81, no. 9, p. 1423–1434.

Murray, B., 2013, Synvolcanic crustal extension during the mid-Cenozoic ignimbrite flare-up in the northern Sierra Madre Occidental, Mexico: Evidence from the Guazapares Mining District region, western Chihuahua: Geosphere, v. 9, no. 5, p. 1201–1235. doi:10.1130/GES00862.1.

Ocampo-Díaz, Y.Z.E., Talavera-Mendoza, O., Jenchen, U., Valencia, V.A., Medina-Ferrusquia, H.C., and Guerrero-Suastegui, M., 2014, Procedencia de la Formación La Casita y la Arcosa Patula: Implicaciones para la evolución tectono-magmática del NE de México entre el Carbonífero y el Jurásico:: Revista Mexicana de Ciencias Geológicas, v. 31, p. 45–63.

Orozco-Esquivel, M.T., Nieto Samaniego, A.F., and Alaniz-Alvarez, S.A., 2002, Origin of rhyolitic lavas in the Mesa Central, Mexico, by crustal melting related to extension: Journal of Volcanology and Geothermal Research, v. 118, p. 37–56. doi:10.1016/S0377-0273(02)00249-4.

Oviedo-Patron, E.G., Aranda-Gomez, J.J., Chavez-Cabello, G., Milona-Garza, R.S., Iriondo, A., Gonzalez-Becerra, P.C., Cervantes-Corona, J.A., and Solorio-Munguia, J.G., 2010, Tectónica de la sierra Cuesta El Infierno y su posible relación con fallas reactivadas cerca del levantamiento de Plomosas, Chihuahua, México: Revista Mexicana de Ciencias Geológicas, v. 27, no. 3, p. 389–411.

Paz Moreno, F.A., Demant, D., Cocheme, J.J., Dostal., J., and Montigny, R., 2003, The Quaternary Moctezuma volcanic field: A tholeiitic to alkali basaltic episode in the central Sonoran Basin and Range province, México: Special paper-Geological Society of America, p. 439–455.

Pearce, J.A., Harris, N.B.W., and Tindle, A.G., 1984, Trace element discrimination diagrams for the tectonic interpretation of granitic rocks: Journal of Petrology, v. 25, p. 956–983. doi:10.1093/petrology/25.4.956.

Peccerillo, A., and Taylor, S.R., 1976, Geochemistry of Eocene calc-alkaline volcanic rocks from the Kastamonu area, northern Turkey: Contributions to Mineralogy and Petrology, v. 58, p. 63–81. doi:10.1007/BF00384745.

Peck, R.E., 1948, A triassic crinoid from Mexico: Palaeontology, v. 22, no. 1, p. 81.

Poole, F.G., Perry Jr., W.J., Madrid, R.J., and Amaya-Martínez, R., 2005, Tectonic synthesis of the Ouachita-Marathon-Sonora orogenic margin of southern Laurentia: Stratigraphic and structural implications for timing of deformational events and plate-tectonic model, *in* Anderson, T.H., *et al.*, eds., The Mojave-Sonora megashear hypothesis: Development, assessment, and alternatives: Geological Society of America Special Paper, v. 393, p. 543–596.

Ramírez, J.C., and Acevedo, C.F., 1957, Notas sobre la geología de Chihuahua: Boletín de la Asociación Mexicana de Geólogos Petroleros, v. 9, no. 9–10, p. 583–770.

Rutter, E.H., 1974, The influence of temperatures, strain rate and interstitial water in the experimental deformation of calcite rocks: Tectonophysics, v. 2, p. 331–334.

Rutter, E.H., 1995, Experimental study of the influence of stress, temperature, and strain on the dynamic recrystallization of Carrara marble: Journal of Geophysical Research, v. 100, p. 24651–24663. doi:10.1029/95JB02500.

Sanchez-Zavala, J.L., Centeno-Garcia, E., and Ortega-Gutiérrez, F., 1999, Review of Paleozoic stratigraphiy of Mexico and its role in the Gondwana-Laurentia connections: Geological Society of America, Special paper, v. 336, p. 211–226.

Simms, M.J., 1986, Contrasting lifestyles in Lower Jurassic crinoids: A comparison of benthic and pseudopelagic isocrinida: Palaeontology, v. 29, no. 3, p. 475–493.

Solari, L.A., Gómez-Tuena, A., Bernal, J.P., Pérez-Arvizu, O., and Tanner, M., 2010, U-Pb Zircon Geochronology with an Integrated LA-ICP-MS Microanalytical Workstation: Achievements in Precision and Accuracy: Geostandards and Geoanalytical Research, v. 34, no. 1, p. 5–18. doi:10.1111/j.1751-908X.2009.00027.x.

Stern, R.J., and Dickinson, W.R., 2010, The Gulf of Mexico is a Jurassic backarc basin: Geosphere, p. 739–754. doi:10.1130/GES00585.1.

Sun, S.-S., and McDonough, W.F., 1989, Chemical and isotopic systematics of oceanic basalts: Implications for mantle composition and processes, *in* Saunders, A.D., and Norry, M.J., eds., Magmatism in the Ocean Basins: London, Geological Society, Special Publications, v. 42, p. 313–345. doi:10.1144/GSL.SP.1989.042.01.19.

Torres, R., Ruiz, J., Patchett, P.J., and Grajales, J.M., 1999, Permo–Triassic continental arc in eastern México: Tectonic implications for reconstructions of southern North America, *in* Bartolini, C., Wilson, J.L., and Lawton, T.F., eds., Mesozoic Sedimentary and Tectonic History of North–Central Mexico: Geological Society of America, Special Paper, v. 340, p. 191–196.

Wells, R.C., 1930, Uraninite from Placer de Guadalupe, Chihuahua: American Mineralogist, v. 15, p. 470–473.